

Tungsten Ligand-Based Sulfur-Atom-Transfer Catalysts: Synthesis, Characterization, Sustained Anaerobic Catalysis, and Mode of Aerial Deactivation

James P. Ward, Patrick J. Lim, David J. Evans, Jonathan M. White, and Charles G. Young*



Cite This: <https://dx.doi.org/10.1021/acs.inorgchem.0c02915>



Read Online

ACCESS |



Metrics & More



Article Recommendations



Supporting Information

ABSTRACT: The synthesis, properties, X-ray structures, and catalytic sulfur-atom-transfer (SAT) reactions of $W_2(\mu-S)(\mu-S_2)(dte)_2(dpde)_2$ (**1**; $dte = S_2CNR_2^-$, where $R = Me, Et, iBu,$ and Bn ; $dpde = S_2C_2Ph_2^{2-}$) and $W_2(\mu-S)_2(dte)_2(dpde)_2$ (**2**) are reported. These complexes represent the oxidized (**1**) and reduced (**2**) forms of anaerobic SAT catalysts operating through the bidirectional, ligand-based half-reaction $(\mu-S)(\mu-S_2) \leftrightarrow (\mu-S)_2 + S^0$. The catalysts are deactivated in air through the formation of catalytically inactive oxo complexes, $(dte)WO(\mu-S)(\mu-dped)W(dte)(dpde)$ (**3**), prompting us to recommend that group 6 SAT activity be assessed under strictly anaerobic conditions.

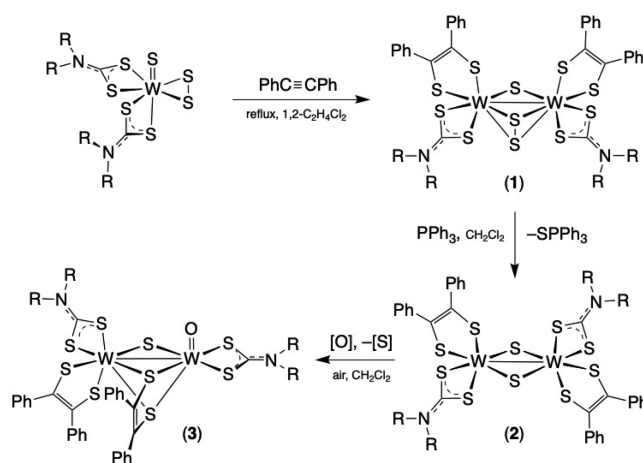
Atom-transfer reactions are an area of fundamental importance in biology, chemical synthesis, and industry, and oxygen-^{1–4} and sulfur-atom-^{4–7} transfers have received much attention. Catalytic atom-transfer technologies are highly prized, and many examples of catalytic oxygen-atom-transfer (SAT) reactions are rare despite reports of unidirectional reactions of this type.^{4–7} Catalytic SAT reactions in group 6 chemistry include the disulfidomolybdenum systems developed by Bargon and co-workers,^{8–10} the sulfidotungsten systems described by Young,¹¹ Sugimoto,¹² and their co-workers,¹³ most of these systems feature monomeric $M(VI) \leftrightarrow M(IV)$ complexes, active sulfido or disulfido ligands, and dithioacid or dithiolene coligands.

Here, we report the synthesis, characterization, and catalytic SAT reactions of dinuclear tungsten(V) complexes containing sulfido, disulfido, dithiocarbamate, and dithiolene ligands (Scheme 1). These complexes, $W_2(\mu-S)(\mu-S_2)(dte)_2(dpde)_2$ (**1**) and $W_2(\mu-S)_2(dte)_2(dpde)_2$ (**2**) ($dte = S_2CNR_2^-$, where $R_{dte} = Me, Et, iBu,$ and Bn ; $dpde = S_2C_2Ph_2^{2-}$), represent the oxidized (**1**) and reduced (**2**) forms of the catalysts, with the bidirectional SAT “half-reaction” being ligand-based rather than metal-based (eq 1). Significantly, both forms of the catalysts have been isolated and unambiguously characterized. Further, the generation of catalytically inactive oxo complexes, $(dte)WO(\mu-S)(\mu-dped)W(dte)(dpde)$ (**3**), is identified as the mode of catalyst deactivation in air. This key result suggests that strictly anaerobic conditions should be maintained in the assessment of group 6 SAT catalysts.



Ink-blue **1** are generated in the reactions of green $WS_2(dte)_2$ and $PhC \equiv CPh$ in refluxing 1,2-dichloroethane under anaerobic conditions (first reaction, Scheme 1). The air-stable complexes were isolated by column chromatography and are

Scheme 1. Summary of Synthetic Transformations



readily soluble in chlorinated solvents and partially soluble in methanol and hydrocarbons. The amelioration of ligand “melting” reactions¹⁵ through the use of a less-activated alkyne is a significant aspect of the syntheses.

Microanalytical and electrospray ionization mass spectrometric results confirmed the formulations of **1**. IR spectra showed a broad, strong $\nu(CN)$ band at $1535\text{--}1500\text{ cm}^{-1}$, while 1H NMR spectra revealed a 1:1 $dte/dped$ ligand ratio and two sets of dte R-group resonances; compounds containing diastereotopic groups exhibited distinctive multiline NMR

Received: October 1, 2020

spectra. ^{13}C NMR spectra revealed resonances assignable to the dtc [$\delta(\text{CS}_2)$ ca. 200] and dped ligands.

Molecules of **1-Me** and **1-Bn** (Figure 1) are dinuclear with severely distorted pentagonal-bipyramidal (PBP) tungsten(V)

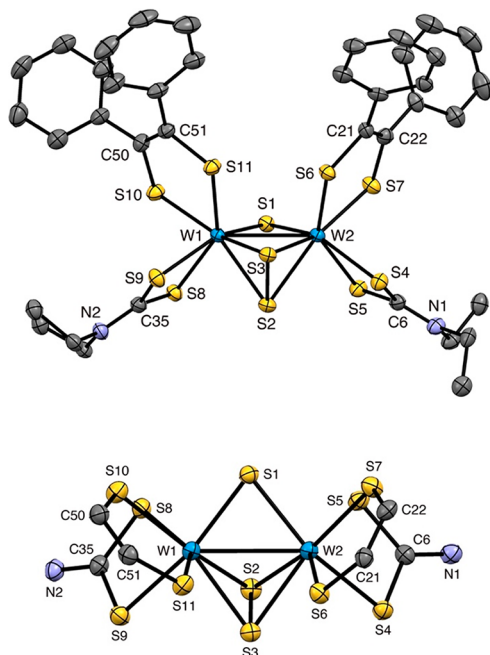


Figure 1. Structure of **1-Bn**. Top: Partial structure showing only the benzylic and phenyl C1 atoms of the dtc Bn groups. Bottom: Core unit viewed perpendicular to the W1–W2–S1–S3 plane. Additional bond distances (Å): W1–S1, W1–S2, W1–S3, W1–S8, W1–S9, W1–S10, and W1–S11 = 2.316(1), 2.490(1), 2.431(1), 2.531(1), 2.500(1), 2.453(1), and 2.365(1), respectively; W2–S1, W2–S2, W2–S3, W2–S4, W2–S5, W2–S6, and W2–S7 = 2.348(1), 2.503(1), 2.432(1), 2.500(1), 2.518(1), 2.357(1), and 2.435(1), respectively. All thermal ellipsoids drawn in this paper are at the 50% probability level.

centers bridged by sulfido and disulfido ligands and coordinated by bidentate dtc and dped ligands; a pseudomirror plane containing the bridging sulfur atoms bisects the W–W vector. The W1–W2 distance of 2.8451(3) Å and the diamagnetism of these formally W(V) d^1 complexes are indicative of W–W bonding (likewise for **2** and **3**).

In **1-Bn**, the PBP geometry of W1 is defined by equatorial atoms S2, S3, S8, S10, and S11 and axial atoms S1 and S9. For W2, atoms S2, S3, S5, S6, and S7 occupy equatorial sites, while S1 and S4 occupy axial sites. The W1 and W2 atoms lie 0.2491(6) and 0.2022(6) Å out of their respective equatorial planes, each with mean sulfur-atom displacements of 0.19 and 0.24 Å, respectively, in the direction of the μ -sulfido ligand S1. The disparate bite angles of the disulfido (ca. 49°) and dped (ca. 79°) ligands account for the major deviations from the ideal PBP equatorial angle of 72°. The axial atoms lie off the perpendiculars to the pentagonal planes by ca. 15°.

The W1, W2, S1, and S3 atoms are nearly planar with a mean atom displacement of 0.053 Å, with atom S2 lying 1.781(3) Å out of this plane. The W– μ -sulfido distances average at 2.33 Å, while the in-plane and out-of-plane W– μ -disulfido distances average 2.43 and 2.495 Å, respectively. The S2–S3 distance of 2.025(2) Å is typical of disulfido ligands. Structurally characterized complexes containing the $[\text{W}_2(\mu\text{-S})(\mu\text{-S}_2\text{-}\kappa^2\text{S},\text{S}')]^6+$ core are rare, with the only other example being the

anion of $(\text{PPh}_4)_2[\text{W}_2(\mu\text{-S})(\mu\text{-S}_2)\text{Br}_8]$.¹⁶ A related molybdenum complex, $\text{Mo}_2(\text{NC}_6\text{H}_3i\text{Pr}_2\text{-2,6})_2(\mu\text{-S})(\mu\text{-S}_2)(\text{dtc})_2$ ($R_{\text{dtc}} = \text{Et}$), has been reported by Coffey and Hogarth.¹⁷

The dped ligand S_2C_4 frameworks are close to planar, with mean atom displacements (and S···S fold angles) of 0.004 Å (0.9°) and 0.007 Å (5.7°) for the ligands containing S6 and S10, respectively. The dtc ligand S_2CNC_2 frameworks are also planar, with the corresponding parameters being 0.0218 Å (13.5°) and 0.0521 Å (8.3°) for the ligands containing S4 and S8, respectively. The metrical parameters for the bidentate ligands are in accordance with those reported for dithiocarbamate and fully reduced dithiolene ligands (this is true of all structures reported herein).^{18,19}

Purple-brown **2** are produced in the reactions of **1** with 1 equiv of PPh_3 in dichloromethane under anaerobic conditions (second reaction, Scheme 1); their precipitation from the reaction mixture facilitates isolation by simple filtration. They are surprisingly insoluble in most solvents or sparingly soluble with decomposition in very polar solvents such as dimethyl sulfoxide and *N,N*-dimethylformamide. Aerial reactions with an excess of PPh_3 result in the formation of **3** (vide infra).

Complexes **2** were characterized by microanalysis, IR and NMR spectroscopy, and X-ray crystallography. Their IR spectra were very similar to **1** with $\nu(\text{CN}) \sim 1530\text{--}1500\text{ cm}^{-1}$. The NMR spectra were consistent with centrosymmetric structures and a 1:1 dtc/dped ligand ratio; once again, the diastereotopic groups of the dtc ligands exhibited distinctive multiline resonances.

Dimeric **2-Bn** (Figure 2) exhibits a centrosymmetric structure with two bridging sulfido ligands linking W1 and W1'. This produces a structure with a planar $\text{W}_2(\mu\text{-S})_2$ unit and symmetry-related dtc and dped ligands on each tungsten. Interestingly, the

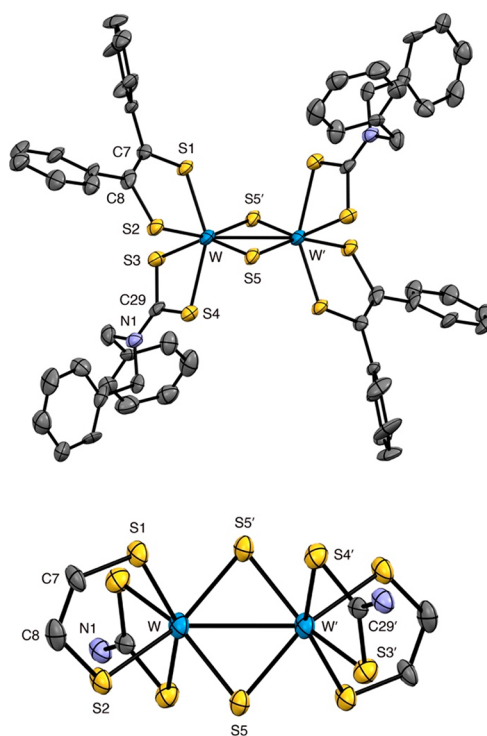


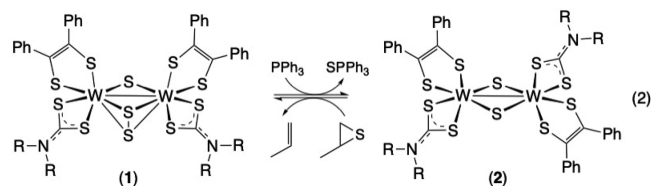
Figure 2. Structure of **2-Bn**. Top: Complete centrosymmetric structure. Bottom: Core unit viewed perpendicular to the $\text{W}_2(\mu\text{-S})_2$ plane. Additional bond distances (Å): W–S1, W–S2, W–S3, and W–S4 = 2.360(3), 2.401(3), 2.493(4), and 2.487(3), respectively.

disposition of the organic ligands has changed significantly compared to **1**-Bn, undergoing an approximate 90° twist around the W–W bond. The tungsten centers display a coordination geometry halfway between octahedral and trigonal-prismatic (TP), with the TP triangular faces, viz., S1,S3,S5 and S2,S4,S5', being related by a trigonal twist of ca. 30°.¹⁸ The W–W vector bisects the S5...S5' edge of the TP structure. Additional distortions from ideal geometries arise from the disparate bite angles of the dtc and dped ligands.

The W–W distance of 2.8919(12) Å and the W–μ-S distances of 2.343(3) and 2.360(3) Å are comparable to those observed in related complexes (vide infra). There is a slight asymmetry in the W–S distances within the dtc and dped ligands, with the longer bonds being roughly trans to the W–μ-S bonds. Similarly, the C–S bonds fall into two groups, with the marginally shorter bond for each ligand being adjacent to the longer W–S bond. The dtc and dped ligands are essentially planar with marginal fold angles.

The [W₂(μ-S)₂]⁶⁺ core is relatively common, and structurally characterized dithiolene complexes include (NEt₄)₂[W₂(μ-S)₂(dped)₄],²⁰ (NEt₄)₂[W₂(μ-S)₂(dmed)₄] (dmed = S₂C₂Me₂²⁻),²¹ (cat)₂[W₂(μ-S)₂{S₂C₂(CO₂Me)₂}]₄ (cat = NnPr₄⁺²² and NEt₄⁺²³), and {(Ph₃P)₂N}₂[W₂(μ-S)₂{S₂C₂(CN)₂}]₄.²⁴ None of these complexes appear to have been tested for SAT activity.

Complexes **1** catalyze SAT from propylene sulfide to triphenylphosphine according to eq 2 (cf. eq 1). The



involvement of **2** is demonstrated by their independent synthesis (vide supra); however, they are less effective starting catalysts because of their limited solubility.

The progress of the SAT reactions catalyzed by **1** were monitored by ³¹P NMR spectroscopy, and typical results are shown in Figure 3. The samples monitored were 5 mol % in catalyst and 100 and 140 mM in PPh₃ and propylene sulfide, respectively, in CDCl₃. The spectra showed a decrease in the concentration of PPh₃ and a concomitant increase in the concentration of SPPH₃ at the turnovers and percent conversions indicated in Table 1. The reactions involving the bulkier dithiocarbamates reached ca. 80–85% completion, but the benzyl derivative achieved complete conversion of PPh₃ to SPPH₃. The methyl derivative was a slower and less stable/reliable catalyst perhaps because of the reduced steric protection of the dinuclear core against adventitious reagents. In other cases, the catalysts remained active under anaerobic conditions, and the addition of more PPh₃ and propylene sulfide led to the further production of SPPH₃.

Catalytic SAT slowed and then ceased upon exposure of the anaerobic reaction mixtures to air. This was accompanied by the formation of OPPh₃ (ca. 10%) and green **3**, with the latter being isolated by column chromatography (R_f ~ 0.4 in 9:1 CH₂Cl₂/*n*-hexane). Green **3** also formed when **1** was reacted with PPh₃ in air. These complexes result from the net exchange of a sulfido ligand in **2** for an oxo ligand (third reaction, Scheme 1); significantly, their formation is identified as the key mode of catalyst deactivation in air.

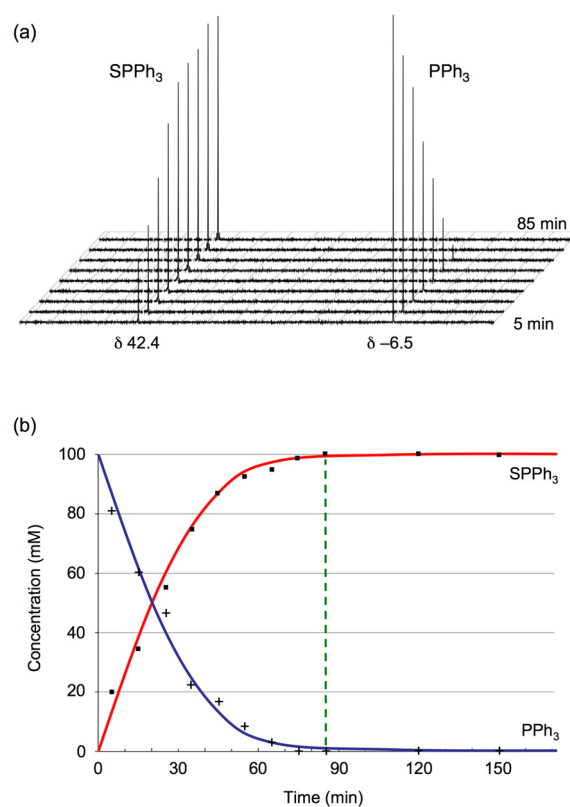


Figure 3. Catalysis of SAT from propylene sulfide to PPh₃ using **1**-Bn. (a) ³¹P{¹H} NMR spectra recorded during monitoring of the reaction from 5 to 85 mins at 10 min intervals. (b) Plot of the change in the concentration of PPh₃ (+) and SPPH₃ (■) with time. The spectra in part a yield the data points shown to the left of the dashed green line (with two representative data points thereafter).

Table 1. Turnover and Conversion for SAT Reactions

derivative	turnover (mol/mol cat/h)	conversion (%)
Me	5.3	50
Et	9.7	80
<i>i</i> Bu	11.7	85
Bn	17.1	100

Complexes **3** exhibited IR spectra very similar to **1** and **2** but with the addition of a ν(W=O) band at 945 cm⁻¹. Mass spectrometric results showed a strong signal due to the [M + H]⁺ ion of **3**.

Molecules of 3-Et and 3-*i*Bu (Figure 4) exhibit asymmetric structures with two distinctly different tungsten(V) centers bridged by three sulfur atoms from sulfido and bidentate dped ligands. In molecule **1** of 3-*i*Bu, the W–μ-S distances fall into three groups; W–S9 av. 2.364 Å < W–S3 av. 2.504 Å < W1–S4 = 2.530(2) Å and W2–S4 = 2.6094(18) Å. The last two sets of bonds are lengthened by the organic nature of the ligand and, in the case of W2–S4, the trans influence of the terminal oxo ligand.^{25,26} The W–W distance is 2.8236(5) Å.

The coordination geometries of both tungsten atoms are highly distorted. That of W1, defined by bidentate dtc and dped ligands and bridging sulfido and dped ligands, is approximately capped TP, with S5 as the capping atom. The dtc and nonbridging dped ligands are nearly symmetrically coordinated and essentially planar. However, both exhibit substantial ligand fold angles of 6.5° and 22.5°, respectively.

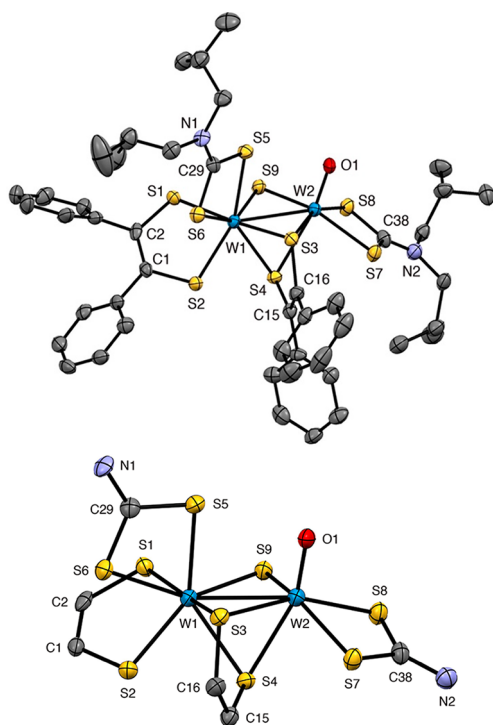


Figure 4. Structure of molecule 1 (of 2) of 3-*i*Bu. Top: Full structure. Bottom: Core unit. Additional bond distances (Å): W1–S1, W1–S2, W1–S3, W1–S5, W1–S6, and W1–S9 = 2.363(2), 2.392(2), 2.513(2), 2.523(2), 2.536(2), and 2.369(2), respectively; W2–S3, W2–S7, W2–S8, and W2–S9 = 2.496(2), 2.459(2), 2.444(2), and 2.359(2), respectively.

The distorted octahedral coordination sphere of W2 is defined by a terminal oxo ligand, a bidentate dtc ligand, and the sulfur atoms of the bridging sulfido and dped ligands. The W2–O1 distance of 1.695(6) Å and the significant trans lengthening of W2–S4 (vide supra) are typical of multiply bonded W=O moieties.^{25,26} The essentially planar dtc framework, also coplanar with W2, is swiveled slightly away from the bulky dped bridging ligand. The bridging dped ligand is slightly distorted from planarity but is close to symmetrical with respect to internal metrical parameters. The core unit of **3** is closely related to that of the recently reported (NEt₄)₂[(WO(dmed))₂(μ-S)(μ-dmed)].²⁷

Catalytic SAT in the MoO(S₂)(dtc)₂ (R_{dtc} = Et) system described by Bargon and co-workers¹⁰ is adversely impacted by the formation of an inactive dimeric oxomolybdenum(V) complex. Here, SAT from MoO(S₂)(dtc)₂ to the substrate is proposed to form MoOS(dtc)₂, which then dimerizes to form Mo₂O₂(μ-S)₂(dtc)₂ with concomitant elimination of thiuram disulfide. In our system, the new W=O ligand could originate from autoxidation of a sulfido ligand, forming intermediate sulfur oxide species^{28,29} with eventual transfer of an oxo equivalent to tungsten, or through hydrolysis of a sulfido ligand. We have been unable to ascertain the origin of the oxo group through spiking experiments. Whatever the source of the oxo group, it is clear that the generation of **3** results in deactivation of the SAT catalysts. On the basis of these results, we propose that catalyst deactivation via the formation of thermodynamically stable, catalytically inactive oxo species is an intrinsic limitation of molybdenum/tungsten-based SAT catalysis and that protection from air may be a general requirement for sustained catalytic SAT in these systems.

In conclusion, the novel mixed-ligand tungsten(V) complexes **1** and their reduced, desulfurized counterparts **2** catalyze SAT from propylene sulfide to triphenylphosphine according to eq 2. These complexes represent the oxidized (**1**) and reduced (**2**) forms of a ligand-based SAT system that does not involve any formal oxidation state changes at the metal centers, with the bidirectional catalyst-based “half-reaction” being given by eq 1. Catalyst deactivation in air, associated with the formation of catalytically inactive **3**, prompts us to recommend the maintenance of anaerobic conditions in studies of group 6 SAT catalysis. Extension to other substrates and refinement of this system through, e.g., the incorporation of chiral dtc or related dithioacid ligands, should expand functionality and facilitate the development of catalysts for asymmetric SAT.

■ ASSOCIATED CONTENT

Supporting Information

The Supporting Information is available free of charge at <https://pubs.acs.org/doi/10.1021/acs.inorgchem.0c02915>.

Syntheses and analytical and spectroscopic data (PDF)

Accession Codes

CCDC 2019209–2019213 contain the supplementary crystallographic data for this paper. These data can be obtained free of charge via www.ccdc.cam.ac.uk/data_request/cif, or by emailing data_request@ccdc.cam.ac.uk, or by contacting The Cambridge Crystallographic Data Centre, 12 Union Road, Cambridge CB2 1EZ, UK; fax: +44 1223 336033.

■ AUTHOR INFORMATION

Corresponding Author

Charles G. Young – Department of Chemistry and Physics, La Trobe Institute of Molecular Sciences, La Trobe University, Melbourne, Victoria 3086, Australia; orcid.org/0000-0002-4019-9961; Email: charles.young@latrobe.edu.au

Authors

James P. Ward – School of Chemistry, University of Melbourne, Victoria 3010, Australia

Patrick J. Lim – Department of Chemistry, University of San Carlos, Cebu City, Philippines

David J. Evans – School of Chemistry, University of Melbourne, Victoria 3010, Australia

Jonathan M. White – School of Chemistry and Bio21 Molecular Science and Biotechnology Institute, University of Melbourne, Victoria 3010, Australia; orcid.org/0000-0002-0707-6257

Complete contact information is available at:

<https://pubs.acs.org/10.1021/acs.inorgchem.0c02915>

Notes

The authors declare no competing financial interest.

■ ACKNOWLEDGMENTS

We thank Ms. Sioe See Volaric and Drs. Christian J. Doonan, Ryan J. Gilbert-Wilson, Victor W.-L. Ng, and Michelle K. Taylor for experimental assistance. We gratefully acknowledge the financial support of the Australian Research Council.

■ DEDICATION

Dedicated to Prof. John H. Enemark on the occasion of his 80th birthday and in recognition of his significant contributions to inorganic and bioinorganic chemistry.

REFERENCES

- (1) Holm, R. H. Metal-centered Oxygen Atom Transfer Reactions. *Chem. Rev.* **1987**, *87* (6), 1401–1449.
- (2) Holm, R. H.; Donahue, J. P. A Thermodynamic Scale for Oxygen Atom Transfer Reactions. *Polyhedron* **1993**, *12* (6), 571–589.
- (3) Young, C. G. Biomimetic Chemistry of Molybdenum. In *Biomimetic Oxidations Catalyzed by Transition Metal Complexes*; Meunier, B., Ed.; Imperial College Press: London, 2000; pp 415–459.
- (4) Woo, L. K. Intermetal Oxygen, Sulfur, Selenium, and Nitrogen Atom Transfer Reactions. *Chem. Rev.* **1993**, *93* (3), 1125–1136.
- (5) Donahue, J. P. Thermodynamic Scales for Sulfur Atom Transfer and Oxo-for-Sulfido Exchange Reactions. *Chem. Rev.* **2006**, *106* (11), 4747–4783.
- (6) Liu, H.; Jiang, X. Transfer of Sulfur: From Simple to Diverse. *Chem. - Asian J.* **2013**, *8* (11), 2546–2563.
- (7) Young, C. G. Models for the Xanthine Oxidase Family of Enzymes. In *Molybdenum and Tungsten Enzymes: Bioinorganic Chemistry*; RSC Metallobiology Series 6; Hille, R., Schulzke, C. E., Kirk, M. L., Eds.; Royal Society of Chemistry: Cambridge, U.K., 2017; pp 194–238.
- (8) Adam, W.; Bargon, R. M. Molybdenum-catalyzed Episulfidation of (*E*)-Cycloalkenes with Elemental Sulfur. *Chem. Commun.* **2001**, 1910–1911.
- (9) Adam, W.; Bargon, R. M.; Bosio, S. G.; Schenk, W. A.; Stalke, D. Direct Synthesis of Isothiocyanates from Isonitriles by Molybdenum-Catalyzed Sulfur Transfer with Elemental Sulfur. *J. Org. Chem.* **2002**, *67* (20), 7037–7041.
- (10) Adam, W.; Bargon, R. M.; Schenk, W. A. Direct Episulfidation of Alkenes and Allenes with Elemental Sulfur and Thiiranes as Sulfur Sources, Catalyzed by Molybdenum Oxo Complexes. *J. Am. Chem. Soc.* **2003**, *125* (13), 3871–3876.
- (11) Eagle, A. A.; Gable, R. W.; Thomas, S.; Sproules, S. A.; Young, C. G. Sulfur Atom Transfer Reactions of Tungsten(VI) and Tungsten(IV) Chalcogenide Complexes. *Polyhedron* **2004**, *23* (2–3), 385–394.
- (12) Sugimoto, H.; Tajima, R.; Sakurai, T.; Ohi, H.; Miyake, H.; Itoh, S.; Tsukube, H. Reversible Sulfurization–Desulfurization of Tungsten Bis(dithiolene) Complexes. *Angew. Chem., Int. Ed.* **2006**, *45* (21), 3520–3522.
- (13) Farrell, W. S.; Zavalij, P. Y.; Sita, L. R. Catalytic Production of Isothiocyanates via a Mo(II)/Mo(IV) Cycle for the “Soft” Sulfur Oxidation of Isonitriles. *Organometallics* **2016**, *35* (14), 2361–2366.
- (14) Pan, W.-H.; Halbert, T. R.; Hutchings, L. L.; Stiefel, E. I. Ligand and Induced Internal Redox Transfer Pathways to New Mo–S and W–S Dithiocarbamate Complexes. *J. Chem. Soc., Chem. Commun.* **1985**, 927–929.
- (15) Lim, P. J.; Cook, V. C.; Doonan, C. J.; Young, C. G.; Tiekink, E. R. T. Transformations Leading to the Generation of Dithiolene Ligands Initiated by Reactions of Sulfur-Rich $WS_2(S_2CNR_2)_2$ Complexes with Dimethyl Acetylenedicarboxylate and Phenylacetylene. *Organometallics* **2000**, *19* (26), 5643–5653.
- (16) Klingelhöfer, P.; Müller, U. Synthesis and Structure of μ -Sulfido- μ -disulfido-octabromoditungsten(V) Ions $[W_2S_3Br_8]^{2-}$. *Z. Anorg. Allg. Chem.* **1986**, *542* (11), 7–12.
- (17) Coffey, T. A.; Hogarth, G. Synthesis and Structure of $[Mo_2(NR)_2(\eta^2-S_2CNEt_2)(\mu-S)(\mu-\eta^2-\eta^2-S_2)]$ ($R = 2,6-Pr^i_2C_6H_3$): a Molecular Model for Molybdenum Trisulfide. *Polyhedron* **1997**, *16* (1), 165–169.
- (18) Beswick, C. L.; Schulman, J. M.; Stiefel, E. I. Structures and Structural Trends in Homoleptic Dithiolene Complexes. *Prog. Inorg. Chem.* **2004**, *52*, 55–110.
- (19) Hogarth, G. Transition Metal Dithiocarbamates: 1978–2003. *Prog. Inorg. Chem.* **2005**, *53*, 71–561.
- (20) Goddard, C. A.; Holm, R. H. Synthesis and Reactivity Aspects of the Bis(dithiolene) Chalcogenide Series $[W^{IV}Q(S_2C_2R_2)_2]^{2-}$ ($Q = O, S, Se$). *Inorg. Chem.* **1999**, *38* (23), 5389–5398.
- (21) Sung, K.-M.; Holm, R. H. Substitution and Oxidation Reactions of Bis(dithiolene)tungsten Complexes of Potential Relevance to Enzyme Sites. *Inorg. Chem.* **2001**, *40* (18), 4518–4525.
- (22) Umakoshi, K.; Nishimoto, E.; Sokolov, M.; Kawano, H.; Sasaki, Y.; Onishi, M. Synthesis, Structure, and Properties of Sulfido-bridged Dinuclear Tungsten(V) Complex of Dithiolene, $(Pr_4N)_2[W_2(\mu-S)_2\{S_2C_2(CO_2Et)_2\}_4]$. *J. Organomet. Chem.* **2000**, *611* (1–2), 370–375.
- (23) Mallard, A.; Simonnet-Jégat, C.; Lavanant, H.; Marrot, J.; Sécheresse, F. Reactivity of Tetrathiometalates with Alkynes. Synthesis and Characterisation of Dithiolene Complexes of Mo, W, and V by ESMS and XRD. *Transition Met. Chem.* **2008**, *33* (2), 143–152.
- (24) Majumdar, A.; Mitra, J.; Pal, K.; Sarkar, S. Mono-oxo Bis(dithiolene) Mo(IV)/W(IV) Complexes as Building Blocks for Sulfide Bridged Bi- and Tri-Nuclear Complexes. *Inorg. Chem.* **2008**, *47* (12), 5360–5364.
- (25) Nugent, W. A.; Mayer, J. M. *Metal–Ligand Multiple Bonds*; Wiley: New York, 1988.
- (26) Parkin, G. Terminal Chalcogenido Complexes of the Transition Metals. *Prog. Inorg. Chem.* **2007**, *47*, 1–165.
- (27) Seo, J.; Shearer, J.; Williard, P. G.; Kim, E. Reactivity of a Biomimetic W(IV) Bis-dithiolene Complex with CO_2 Leading to Formate Production and Structural Rearrangement. *Dalton Trans* **2019**, *48* (47), 17441–17444.
- (28) Manoli, J.-M.; Brégeault, J.-M.; Potvin, C.; Chottard, G. Structural and Spectroscopic Studies of the $[Mo_2(\mu_4-S_2)(\mu_2-SO_2)(CN)_8]^{4-}$ Anion, a Complex With a Mo–Mo Bond and a Distorted Confacial Bis-bipyramidal Framework. *Inorg. Chim. Acta* **1984**, *88* (1), 75–81.
- (29) Kubas, G. J. Chemical Transformations and Disproportionation of Sulfur Dioxide on Transition Metal Complexes. *Acc. Chem. Res.* **1994**, *27* (7), 183–190.